Palm print recognition system using siamese network and transfer learning

Aml Fawzy [1], Mohamed Ezz [2, *], Sayed Nouh [1], Gamal Tharwat [1]

[1]Systems and Computer Engineering Department, Faculty of Engineering, Al-Azhar University, Cairo, Egypt
[2]College of Computer and Information Sciences, Jouf University, Sakaka, Saudi Arabia

ABSTRACT

This paper proposes a palmprint authentication approach using a one-shot learning technique based on similarity instead of classification (used by most other proposals). The one-shot learning technique uses the siamese network architecture built on top of the pre-trained VGG16 to efficiently reduce the cost and time of training the siamese network. This technique allows the user registration using only one palmprint and then performs the authentication process by performing a siamese similarity measure instead of classification techniques. The proposed model achieved high accuracies scores of 97%, 96.7% for Tongji datasets, 92.3%, 91.9% for PolyU-IITD datasets, 90.9%, 88.3% for CASIA datasets and 95.5% for COEP dataset. These performances were measured based on the testing dataset for unseen persons while the siamese training dataset was applied to different persons. The proposed model uses the pre-trained part of VGG16 as a feature extraction part then feeds the generated feature vector into the Euclidean distance layer that is trained in conjunction with the sigmoid layer to output the final similarity decision. Compared to other models, this proposed model achieved a high average accuracy of 93.2% and 0.19 EER over the available four palm print datasets which is generalized over proposals. All codes are open-source and available online at https://github.com/ProjectsRebository/PalmPrint-recognition-using-Transfer-Learning.

1. Introduction

In the last 40 years, automatic computer-based biometric identification has emerged as a strong technique for recognizing an individual's identity. The biometric characteristics derived from human biological organs; such as iris, retina, face, and various hand patterns; including fingerprint, finger knuckle pattern, hand geometry, Palm Print, etc., are grouped as physiological characteristics, while others are called behavioral characteristics; such as gait, voice, eye blinking (Saied et al., 2020), lip movement (Ezz et al., 2020) signature, and gesture (Wang and Geng, 2009; Kumar and Srinivasan, 2012; Abdelwhab and Viriri, 2018; Saqib and Kazmi, 2018). Token and/or password-based methods have historically been used for personal authentication.

Their limitations hinder their use. However, these tokens can be stolen or misplaced (Student ID Card), information or passwords (ATM pin or Mail ID) can be guessed or forgotten similarly. On the other hand, many biometric systems are based on biological features, such as iris (Liu et al., 2017), retina, face (Moridani et al., 2020), voice, character, fingerprint (Rivaldería et al., 2017), and DNA, etc. have been successfully developed for many commercial applications due to rapid growth in hardware technology in terms of computing speed and high-resolution capture devices (Kumar and Srinivasan, 2012; Liu et al., 2017). Samsung and numerous other smartphone companies have recently released their mobile variants with biometric protection systems focused on the face and iris. In addition, over the last 4-5 years, fingerprint, face, and iris technologies have also been used in laptops as a safety feature. However, there are still few constraints on biometric systems today, limiting their use and accuracy in civilian and forensic applications. The iris and retina scan systems are costly and extremely sensitive to the slightest body movement. Since the Palm Print texture is more complex and more resistant to

damage and debris, it is tougher than a fingerprint. In addition, a Palm Print meets the basic requirements (Dian and Dongmei, 2016) for personal authentication as a universal, special and permanent biometric pattern because the palm line features; such as palm lines, creases, ridges, minutiae, and delta points, are stable and remain unchanged throughout the life of an individual (Zhang et al., 2012; Kong et al., 2009; Zhang et al., 2017).

2. Literature survey

Palm print attracted many researchers, and their work on Palm Print extraction approaches, rely on CNNs, can be divided into three categories as tabulated in Table 1:

1. Using pre-trained models (on Image Net); the network's output is the extracted feature. A classifier, such as SVM, is also used.
2. Networks of filters that are optimized using different approaches.
3. Training from scratch (or using transfer learning) of DNNs to determine embedding that minimizes intra-class distance and maximizes inter-class distance

Our proposed research presented a system that can directly produce the similarity of two input Palmprint images using the siamese network (Melekhov et al., 2016). We used the pre-trained model VGG16 (Rezende et al., 2018) for feature extraction.

Table 1: Previous related work

Ref.	Approach	Dataset	Accuracy	EER
USING PRE-TRAINED DNNs				
(Ramachandra et al., 2018)	Uses transfer learning (AlexNet (Krizhevsky et al., 2017)) to match Palm Prints acquired from infants. The class decision was obtained by a fusion rule, which considered the SVM prediction and the network Softmax prediction.	CPNB (Genovese et al., 2019)		0.3 %
(Tarawneh et al., 2018)	Several ImageNet pre-trained networks were used (AlexNet, VGG16, and VGG19 (Simonyan and Zisserman, 2015)). The deep features extracted were then matched using a multi-class SVM.	COEP (College of Engineering, Pune-411005 (An Autonomous Institute of Government of Maharashtra). Palmprint Dataset (COEP, 2021)	89.00%	
		MOHI (Ramachandra et al., 2018)	95.5%	
(Dian and Dongmei, 2016)	To extract deep features, it uses AlexNet pre-trained on ImageNet. These were then matched using the distance from Hausdorff.	PolyU II (Kumar, 2018)		0.044 %
		CASIA (Sun et al., 2005)		0.0803%
		IITD (IITD, 2014). IIT Delhi Touch less Palmprint Database (Version 1.0).		0.1113%
(Meraoumia et al., 2017)	PCANet, ScatNet AND PalmNet For Palmprint feature extraction, PCANet was used. Both SVM and KNN were used for classification.	CASIA		0.12%
		HKPU-MS (Zhang et al., 2009)		0.0%
(Genovese et al., 2019)	The PCANet strategy extended to include convolutions in the 2nd layer with fixed-size and variable-size Gabor filters. The defined 'PalmNet' architecture determines the Gabor filters with the highest response, followed by a binarization layer. An alternative architecture, entitled 'PalmNetGaborPCA' is considered, where the first layer filters are tuned using the PCA-based tuning method used in PCANet, while the 2nd layer kernels are configured using the Gabor-based tuning protocol. For classification, a simple KNN classifier is used.	CASIA		0.72%
		IITD		0.52%
		REST (Charfi et al., 2016)		4.50%
		Tongji (Zhang et al., 2017)		0.16%
TRAINING DNNs				
(Izadpanahkakhk et al., 2019)	Four networks trained and tested (GoogleNet, VGG16, VGG19, and a CNN developed by Chatfield for the ImageNet challenge) (GoogleNet, VGG16, VGG19 and a CNN developed by Chatfield for the ImageNet challenge)	SMPD	VGG-16 (90.3%) VGG-19 (91.6%) CNN-F (93.4%) GoogLeNet (92.5)	
(Zhang et al., 2019)	Using a siamese architecture, two MobileNets output feature vectors are then fed to an intra-class probability sub-network (0 for inter-class and 1 for intra-class, with 0.5 as a decision threshold). However, it is not clear which loss feature they used (most likely contrastive loss).	MPD	89.91%	
(Zhong et al., 2018)	Used VGG16 based transfer-learning (initially trained on ImageNet) and Contrastive loss.	XJTU (Shao et al., 2019)		4.559%
		PolyU (Kumar, 2018)		0.2819%

3. Materials and methods

3.1. Datasets

1. PolyU-IITD includes left- and right-hand photographs from more than 230 subjects, with at least 5 hand image samples from each of the hands contributed by all the subjects. Fig. 1 shows samples of this database."

2. CASIA Palmprint Image Database includes 5,502 Palmprint images taken from 312 subject samples shown in Fig. 1. For each subject, Palmprint images were collected from both left and right palms. Both Palmprint images are 8-bit JPEG files at the gray level.
3. The database of COEP consists of 8 separate single-person palm pictures. The database contains a total of 1344 images belonging to 168 individuals. Fig. 1 shows samples of this dataset.

4. Tongji Photos of 300 volunteers, including 192 males and 108 females, were collected. Two different sessions gathered samples. The subject was asked in each session to provide 10 photos for each palm. Therefore, from each subject, 40 images were collected from 2 palms. In total, there are 12,000 photos taken from 600 different palms in the collection. Samples of this dataset showed in Fig. 1.
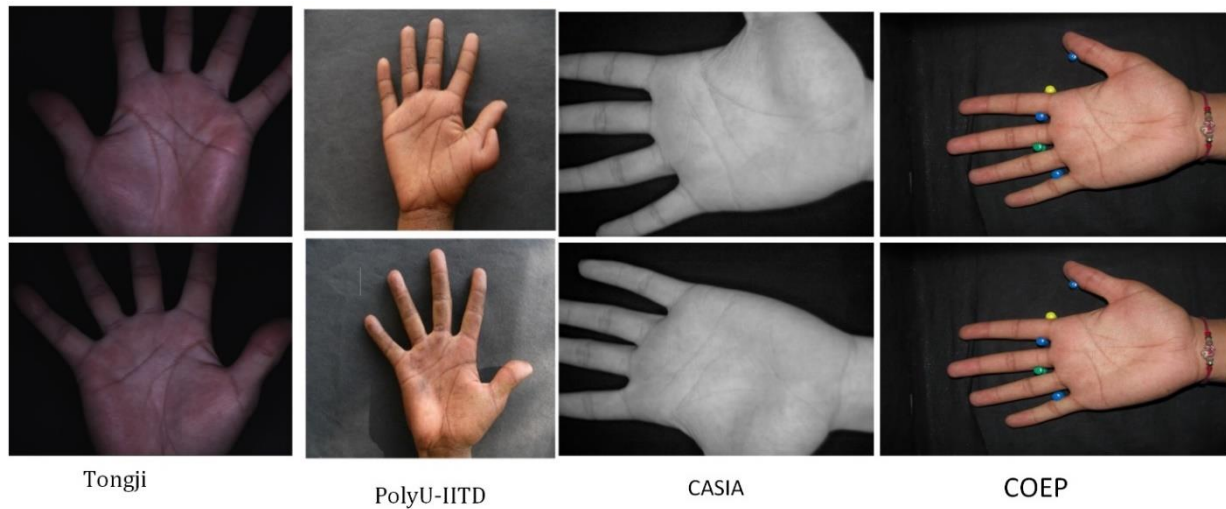
Fig. 1: Dataset samples

3.2. Dataset preparation

For each dataset, downloaded images were in one folder. One of these datasets makes the first ten images for the right hand for the first person, then the second ten images for the left hand for the first person. The other datasets nearly do the same; for example, in one of them, images are named as IMG person number (image number).jpg; for example, IMG_001(1).jpg corresponds to person number 1 and his/her 1st image and so on. The other datasets do the same; however, the only difference is the naming of the image. To prepare these datasets, we made python code to prepare the folder for each person and add each person's images in his folder.

3.3. Transfer learning

Pre-trained models are used in transfer learning as the starting point for computer vision and natural language processing tasks, given the vast computational and time resources needed to develop neural network models on these issues and the enormous skill jumps they provide on related issues. First, a base network trained on a base dataset and task in transfer learning, and then repurposed or transferred the learned features to a second target network to be trained on a target dataset and task. If the features are general, this process will tend to work; meaning that they are suitable for both base and target tasks rather than specific to the base task. The inductive transfer is known as this method of transfer learning used in deep learning. This is whereby using a model suitable for a different but related task, the scope of possible models (model bias) is narrowed in a useful way. By using transfer learning, three potential advantages are:

1. Higher Beginning: On the source model, the initial skill (before optimizing the model) is higher than it would otherwise be.
2. Slope Higher: The rate of ability enhancement during the source model's training is steeper than it would otherwise be.
3. Asymptote Higher: The educated model has converged competence is higher than it would otherwise be.

3.4. Proposed model

We proposed the below network - using one-shot learning this network measures the similarity. Thus, we say that the network predicts the score in one shot, which is the most challenging part of our network. As in a one-shot classification, we require only one training example for each class, which has a great advantage over traditional classification. Our network consists of three main parts: as shown in Fig. 2.

3.4.1. Feature extraction layer: Pre-trained VGG16

For feature extraction, we used the VGG16 pre-trained model; its architecture is shown in Fig. 3. The Pre-trained model was previously trained on ImageNet of 14 million images dataset to classify 1000 object types. The model has a large number of trained parameters for networks. Generally, training such a network is time and resource consuming (Rivaldería et al., 2017; Jain et al., 2004). The VGG network is distinguished by its simplicity, using only 3×3 convolutional layers stacked on top of each other in increasing depth. Reducing volume size done by max-pooling SoftMax classifier (above) is then followed by two completely linked layers, each

with 4,096 nodes (Simonyan and Zisserman, 2015). Our experiment removes the last classification layer (i.e., SoftMax layer) and the output taken from the last feature vector layer (4096), which output the extracted features from the image.
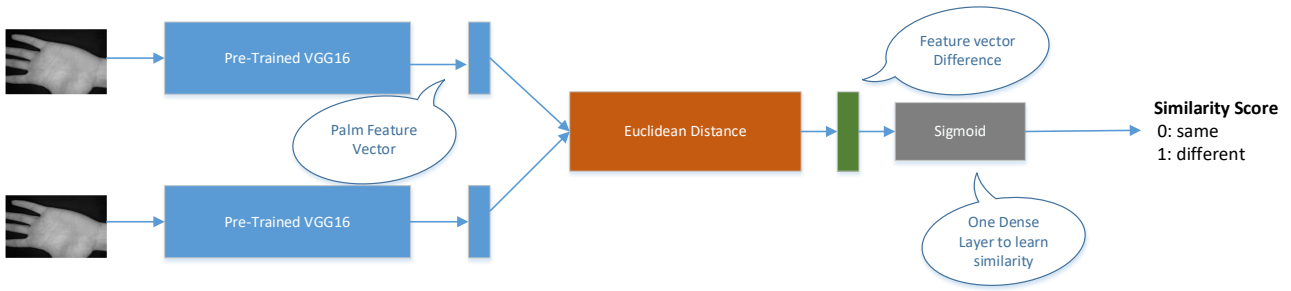
Fig. 2: Our proposed model
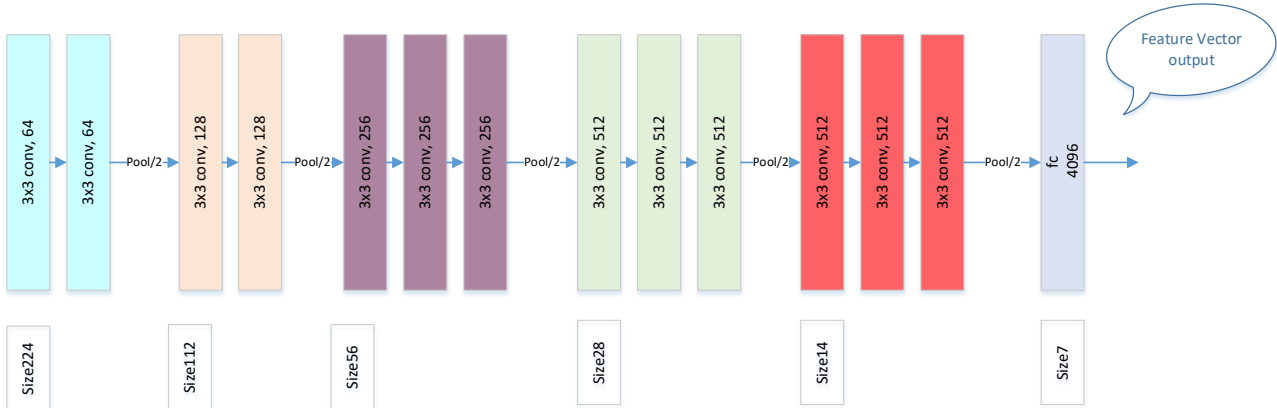
Fig. 3: VGG16 architecture

3.4.2. Similarity measures layer: Using Euclidian distance

After generating features from two images, then we measure the similarity between images by taking the difference between two output vectors using Euclidean distance (Dokmanic et al., 2015), as shown in Eq. 1.

$$d(p,q) = \sqrt{\sum_{i=1}^{n}(q_i - p_i)^2} \qquad (1)$$

3.4.3. Decision layer: Using a sigmoid activation function

As shown in Fig. 4, this layer will be trained to decide whether the two images belong to the same person or a different person. This layer will produce a similarity score that denotes the probability that the two input images belong to the same person or not. Using a sigmoid function as shown in equation 2, the similarity score is usually squished between 0 and 1, where 0 denotes no similarity and 1 denotes complete similarity. Any number from 0 to 1 will be interpreted accordingly. Our model was learning a function of similarity, which takes as input two images and demonstrates how similar they are (Ramachandran et al., 2017). Sigmoid function is:

$$\sigma(z) = \frac{1}{1+e^{-z}} \qquad (2)$$

z is calculated using Eq. 3 which is shown below.

$$z = \sum_{i=1}^{m} w_i x_i + bias \qquad (3)$$

3.5. Traditional classification vs one-shot-learning

Using traditional classification, the input image is fed into a series of layers, and finally, we create a probability distribution over all classes at the output (typically using a SoftMax). Assume that we want to develop a palm recognition system for a small organization with only 10 employees. Using a traditional approach for classification, Dataset samples. There are two main issues for worker identification model building as follows:

a) First needs many different photos for each of the 10 individuals to train such a system that may not be the feasible company has thousands of workers in an organization
b) What if a new worker hired or an existing worker leaves the company? The model has to be re-trained again with every change by increase or decrease the number of output classes. Particularly for large organizations where recruiting and attrition occur almost every week, re-training is not feasible.

3.5.1. Using one-shot-learning

Recently, one-shot learning has found successful applications, including facial recognition and ID checks. Instead of treating the problem as a classification problem, the one-shot learning turns it

into a similarity problem. It helps to solve both traditional classification issues, as it does not take too many instances of a class, and only a few are enough to build a good model. The one-shot learning use architecture called the "siamese network." It takes two images as input and encodes their features

into a set of numbers. The siamese network trains to measure the distance between the features in two input images, as shown in Fig. 5. However, this architecture needs to restructure the dataset to be suitable for a triplet loss function.
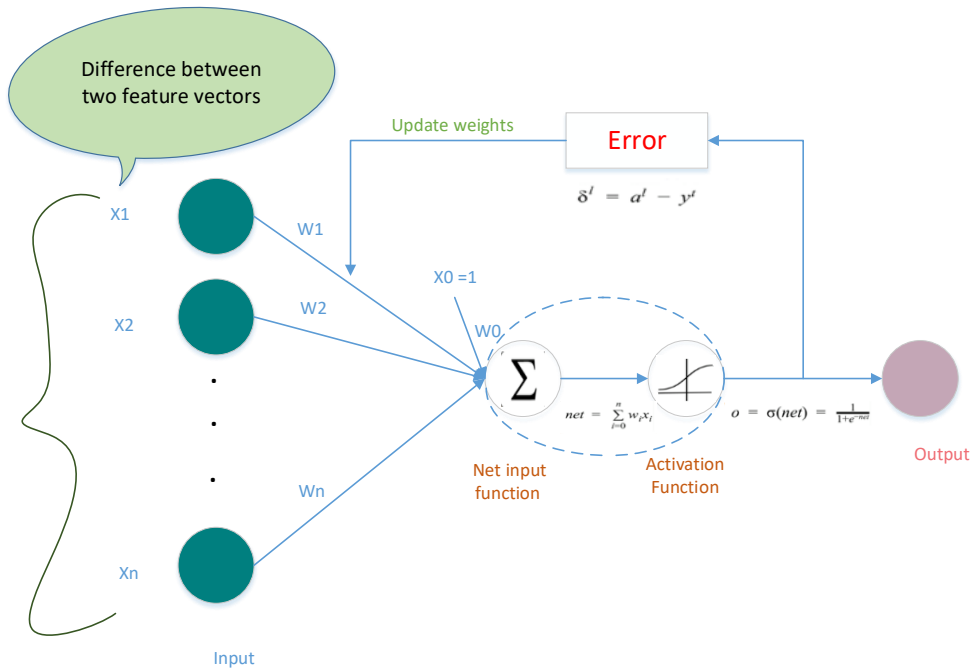
Fig. 4: Sigmoid

These restructures format the data as three images: A person A image (called anchor), another image for person A (called positive image), and a different person B image (called negative image). The siamese network will be trained so that the feature encoding values for the anchor (of person A) and positive image (of person A) are very close, while that of the negative image (of person B) is very different. The training process will use a few images (sample) from persons to train the model while the traditional new thousands of images for each person for train the model. The limitation of the siamese network is sensitive to variations that degrade the accuracy in the face recognition system if the person in one of the images is wearing a hat or glasses, which not the case in palm recognition.

3.6. Performance measures

Using the palm for person recognition, we will need a different measure to evaluate the model performance. Most of the researchers use four different measures. These measures are FAR (false acceptance rate) and FRR (false rejection rate), GAR (Genuine Acceptance Rate), accuracy, and EER (equal error rate). FAR denotes the situation in which an impostor can be marked as an original and is allowed to pass as shown in Eq. 4. FRR denotes the situation in which the initial is rejected, as shown in Eq. 5. GAR denotes the situation in which the initial is accepted, as shown in Eq. 6. The goal is to minimize both FAR and FRR, which EER achieves.

The EER, which calculated using Eq. 7 is the point where FAR and FRR cross; it is the best threshold to pick (Ali et al., 2017) and provides the best accuracy.

$$FAR = \frac{\text{Imposter Score exceeding thershold}}{\text{All Imposter Score}} X100 \quad (4)$$

$$FRR = \frac{\text{Genuine Scores falling below thershold}}{\text{All Genuine Scores}} X100 \quad (5)$$

$$GAR = 1 - FRR \quad (6)$$

$$EER = \frac{FAR+FRR}{2} \quad (7)$$

4. Results and discussion

Our model contains two main parts; the first is VGG16, and the second is the decision network. In our system, we need to train only the decision network. We don't need to train VGG16. We remove the top layer and then use it as a feature extractor. Then, we use these features for training decision networks. When training a decision network, we need to generate pairs (anchor: positive and anchor: negative) of palms to train our network on. So, we arrange it as follows; for example, if a user has 8 images; then we create 28 pairs from the same person as following:

anchor: positive pairs: P11: P12, P11, P13, P11: P14, ... P21: P22, P22: P23, Pn7: Pn8
anchor: negative pairs: P11: Px1y1, P11, Px2y2, P11: Px3y3, ... P12: Px4y4, P12: Px5y5, P17: Px8y8x
Such as the P11: Image 1 of person 1, P23: image 3 of person 2, Pn7: image 7 of person n and the Px1y1: random image x1 of random person y1.
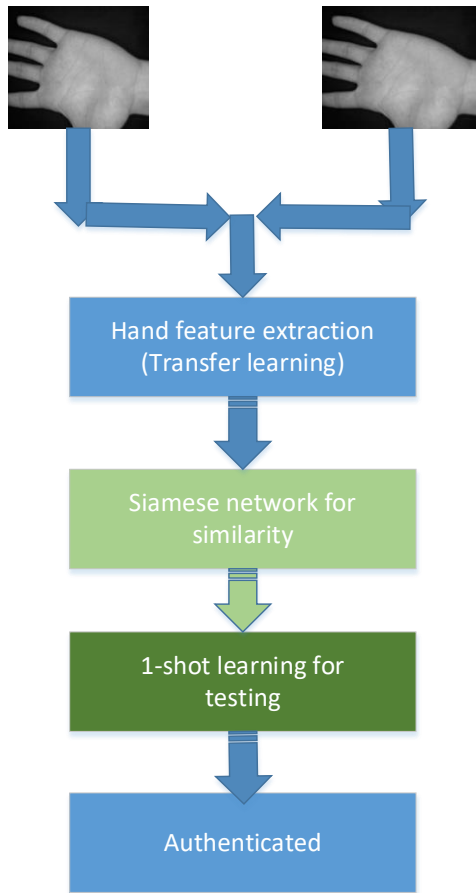
Fig. 5: One-shot classification

In our training experiment, we prepare training and testing and validation set as follows: 70: 15: 15 train, test and validate where the validation used for tunning the model and the test used for scoring the model and the persons we used for validating and test different from persons that the model trained on. The result is shown in Table 2 for the model on the different types of datasets. In the training process, we use early stopping techniques on validation data to get the best model and prevent over fitting.

Fig. 6 shows the accuracy vs. epoch graph of Tongji right and left hand; it can be observed from the figure that the accuracy rate was not rugged; it was steady with a small difference as for right hand, we achieved 97.9%, and for the left hand, we achieved 96.9%. and shows the accuracy vs. epoch graph of PolyU-IITD right and left hand It can be observed from the figure that the accuracy rate was nearly steady may be due to image resolution, with a small difference as for the right hand, we achieved 92.3%, and for the left hand, we achieved 91.9%.and shows the accuracy vs. epoch graph of CASIA right and left hand. It can be observed from the figure that the accuracy rate was steady with a small difference as for the right hand, we achieved 90%, and for the left hand, we achieved 88.3%. Accuracy is less than the previous datasets may be due to this dataset is grayscale images. And shows the accuracy vs. epoch graph of COEB. It can be observed that the accuracy rate was nearly steady. Accuracy for this dataset reaches 95.5%.
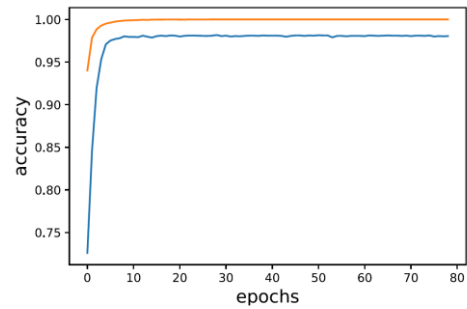
Accuracy vs. epoch graph of Tongji right hand
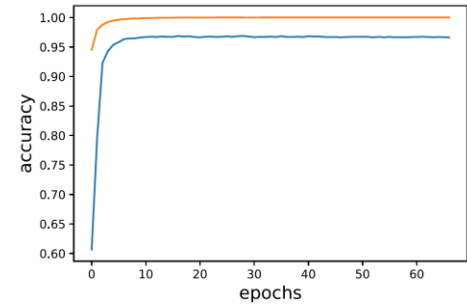
Accuracy vs. epoch graph of Tongji left hand
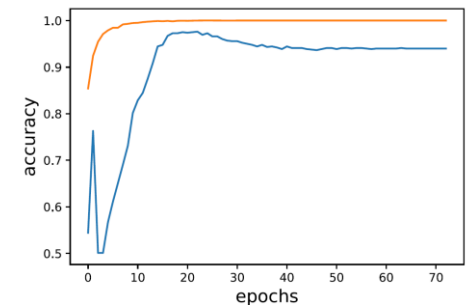
Accuracy vs. epoch graph of PolyU-IITD right hand
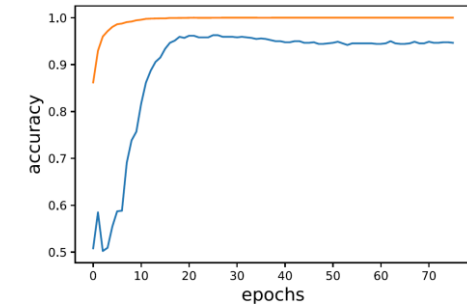
Accuracy vs. epoch graph of PolyU-IITD left hand
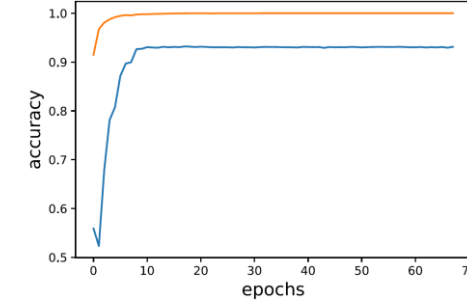
Accuracy vs. epoch graph of CASIA left hand
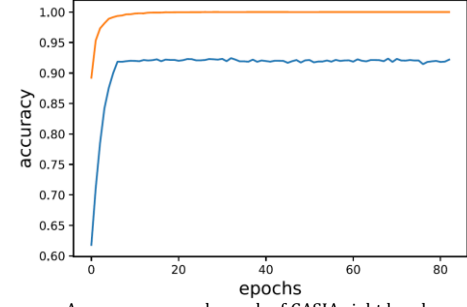
Accuracy vs. epoch graph of CASIA right hand

95
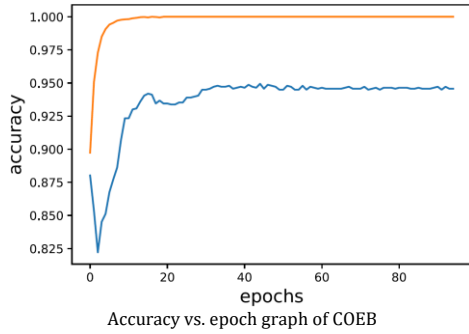
Fig. 6: Accuracy vs. epoch graph (Train: Orange; Test: Blue)

As in Fig. 7 and Table 2, the number of false acceptances (FAR) decreases, the number of false rejections (FRR) will increases, and vice versa. The point where the two lines intersect also has a name: The Equal Error Rate (EER). This is where the percentage of false rejections and false acceptances is the same. The lower EER is for Tongji's left hand and is 0.0264, and the highest is for PolyU-IITD's left hand and is 0.4771.

A plot of the genuine accept rate (GAR) as a FAR function is known as the ROC curve. We compute the GAR and FAR for the different values of t (each setting of t gives us one pair of (GAR, FAR) values and thus corresponds to one point on the ROC curve) provided the classifier scores for each palm pair as in Fig. 8 for the four datasets. Compared to other models that use a similar approach, our accuracy is higher, as shown in Table 3 as the first one that uses siamese with transfer learning (MobileNet) with accuracy reaches 89.91, and the other one uses training from scratch for accuracy vgg16 which is time and resource consuming. Also, our proposed model achieved a high average accuracy of 93.2% and 0.19 EER over the available four palm print datasets.

Tongi left hand EER curve

Tongi right hand EER curve

CASIA left hand EER curve

CASIA right hand EER curve

POLYU left hand EER curve

POLYU right hand EER curve

COEB EER curve
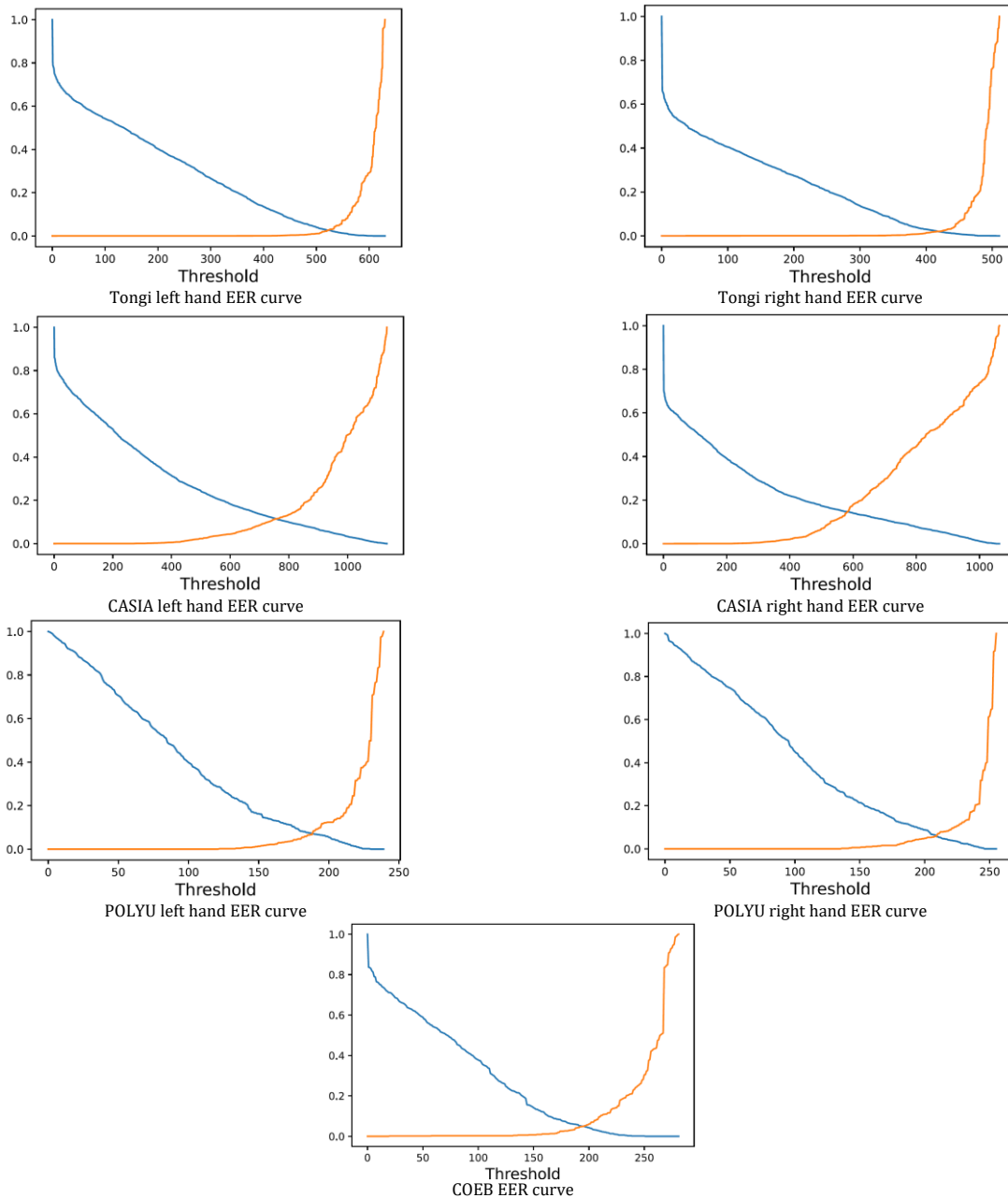
Fig. 7: EER curve (FRR: Orange; Test: FAR)

Table 2: Our model result

Dataset	FAR	FRR	GAR	Accuracy	EER
Tongji right hand	0.0207	0.0207	0.9793	0.979	0.2837
Tongji left hand	0.0266	0.0261	0.9739	0.969	0.0264
PolyU-IITD right hand	0.06274	0.0568	0.9432	0.923	0.2612
PolyU-IITD left hand	0.0764	0.0745	0.9255	0.919	0.4771
CASIA right hand	0.1543	0.1539	0.8461	0.90	0.1541
CASIA left hand	0.1095	0.1091	0.8909	0.883	0.1093
COEP	0.0357	0.0372	0.9628	0.955	0.0364

Tongji left hand ROC curve

Tongji right hand ROC curve

CASIA left hand ROC curve

CASIA right hand ROC curve

PolyU left hand ROC curve

PolyU right hand ROC curve
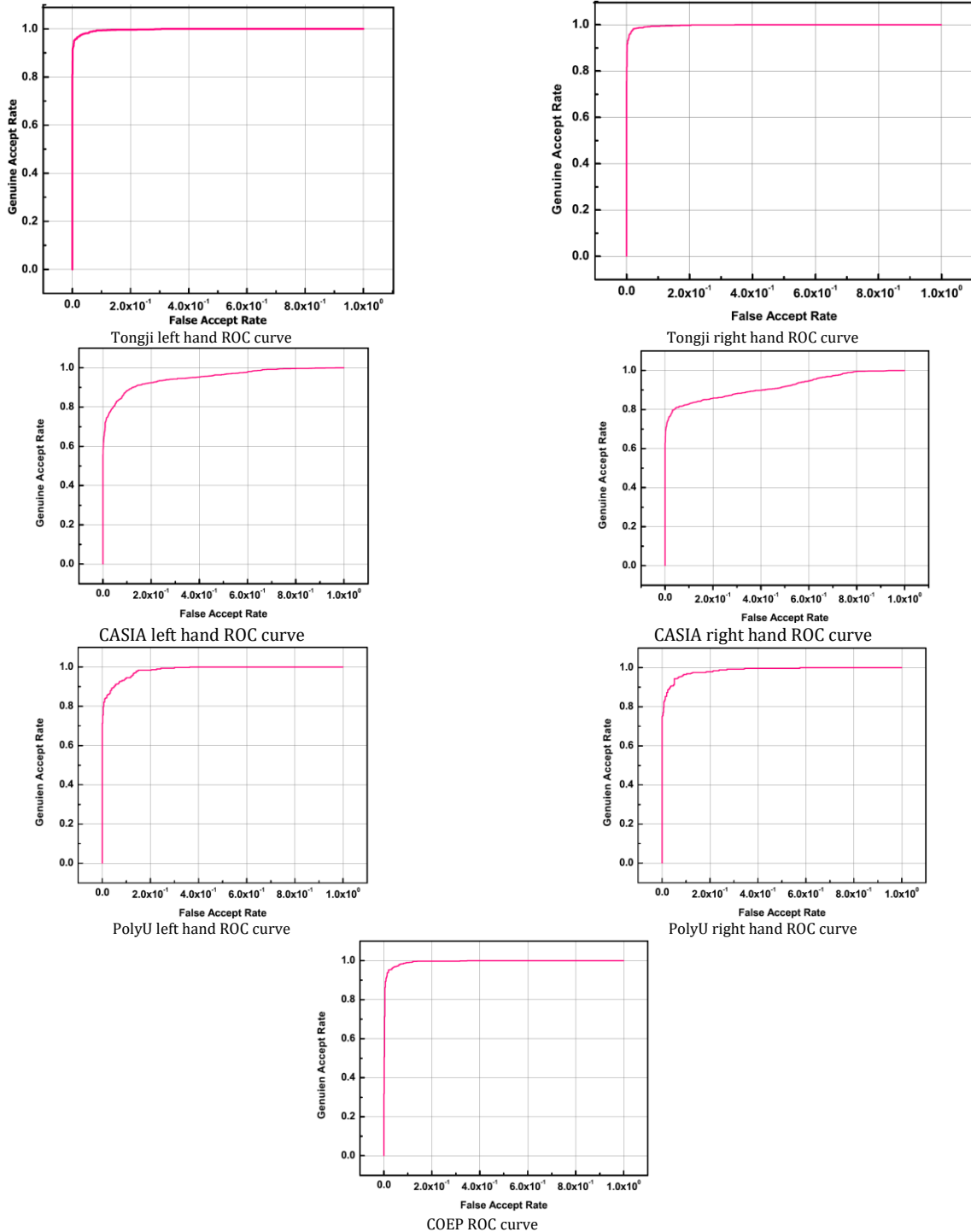
COEP ROC curve

Fig. 8: ROC Curve

5. Conclusion

Using Transfer Learning and Siamese Network, we proposed a Palm Print recognition technique, which can directly extract the similarity of two input Palm Prints. Our proposed model consists of three Parts:

1. Feature extraction layer: Use pre-trained VGG16
2. Similarity measures layer: Use Euclidian distance
3. Decision layer: Use a sigmoid activation function

Our proposed model does not take too many instances of a class, and only a few are enough to build a good model. When we have a new person that we want to add to the model, we now only need a single image for him to be stored on the database to recognize this user, which is the great benefit of our model. We achieved the following performance:

1. 97% for Tongji right-hand dataset and 96.7% for Tongji left-hand dataset.

2. 92.3% for PolyU-IITD right hand dataset and 91.9% for PolyU-IITD.
3. 90.9% for CASIA right hand dataset and 88.3% for CASIA left hand dataset.
4. 95.5% for COEP dataset.

Also, our proposed model achieved a high average accuracy of 93.2% and 0.19 EER over the available four palm print datasets.

Table 3: Comparison between our work and previous work

Ref	Datasets						
	Tongji right hand	Tongji left hand	PolyU-IITD right hand	PolyU-IITD left hand	CASIA right hand	CASIA left hand	COEP
(Tarawneh et al., 2018) (Dian and Dongmei, 2016) (Dian and Dongmei, 2016) (Genovese et al., 2019)	EER=0.16	EER=0.16	EER=0.113 EER=0.52	EER=0.113 EER=0.52	EER=0.0803 EER=0.12 EER=0.72	EER=0.0803 EER=0.12 EER=0.72	Acc =89.00%
Our work	FAR=0.0207 FRR=0.0207 Acc=97.9 EER=0.2837	FAR =0.0266 FRR =0.0261 Acc=96.9 EER=0.0264	FAR =0.06274 FRR =0.0568 Acc=92.3 EER=0.2612	FAR=0.0764 FRR=0.0745 Acc=91.9 EER=0.4771	FAR=0.1543 FRR=0.1539 Acc=90 EER=0.1541	FAR =0.1095 FRR =0.1091 Acc=88.3 EER=0.1093	FAR =0.0357 FRR =0.0372 Acc=95.5 EER=0.0364

Compliance with ethical standards

Conflict of interest

The author(s) declared no potential conflicts of interest with respect to the research, authorship, and/or publication of this article.

References

Abdelwhab A and Viriri S (2018). A survey on soft biometrics for human identification. In: Yang J, Sun PD, Yoon S, Chen Y, and Zhang C (Eds.), Machine learning and biometrics: 37-54. BoD–Books on Demand, Norderstedt, Germany. https://doi.org/10.5772/intechopen.76021

Ali MM, Yannawar PL, and Gaikwad AT (2017). Multi-algorithm of palmprint recognition system based on fusion of local binary pattern and two-dimensional locality preserving projection. Procedia Computer Science, 115: 482-492. https://doi.org/10.1016/j.procs.2017.09.091

Charfi N, Trichili H, Alimi AM, and Solaiman B (2016). Local invariant representation for multi-instance toucheless palmprint identification. In the IEEE International Conference on Systems, Man, and Cybernetics, IEEE, Budapest, Hungary: 003522-003527. https://doi.org/10.1109/SMC.2016.7844778

COEP (2021). COEP palm print database. College of Engineering Pune, Pune, India. Available online at: https://www.coep.org.in/resources/coeppalmprintdatabase

Dian L and Dongmei S (2016). Contactless palmprint recognition based on convolutional neural network. In the IEEE 13th International Conference on Signal Processing, IEEE, Chengdu, China: 1363-1367. https://doi.org/10.1109/ICSP.2016.7878049

Dokmanic I, Parhizkar R, Ranieri J, and Vetterli M (2015). Euclidean distance matrices: Essential theory, algorithms, and applications. IEEE Signal Processing Magazine, 32(6): 12-30. https://doi.org/10.1109/MSP.2015.2398954

Ezz M, Mostafa AM, and Nasr AA (2020). A silent password recognition framework based on lip analysis. IEEE Access, 8: 55354-55371. https://doi.org/10.1109/ACCESS.2020.2982359

Genovese A, Piuri V, Plataniotis KN, and Scotti F (2019). PalmNet: Gabor-PCA convolutional networks for touchless palmprint recognition. IEEE Transactions on Information Forensics and Security, 14(12): 3160-3174. https://doi.org/10.1109/TIFS.2019.2911165

IITD (2014). IIT Delhi touch less palmprint database (Version 1.0). Indian Institute of Technology Delhi, New Delhi, India.

Izadpanahkakhk M, Razavi SM, Taghipour-Gorjikolaie M, Zahiri SH, and Uncini A (2019). Novel mobile palmprint databases for biometric authentication. International Journal of Grid and Utility Computing, 10(5): 465-474. https://doi.org/10.1504/IJGUC.2019.102016

Jain AK, Ross A, and Prabhakar S (2004). An introduction to biometric recognition IEEE transactions on circuits and systems for video technology. Special Issue on Image-and Video-Based Biometrics, 14(1): 4-20. https://doi.org/10.1109/TCSVT.2003.818349

Kong A, Zhang D, and Kamel M (2009). A survey of palmprint recognition. Pattern Recognition, 42(7): 1408-1418. https://doi.org/10.1016/j.patcog.2009.01.018

Krizhevsky BA, Sutskever I, and Hinton GE (2017). ImageNet classification with deep convolutional neural networks. Communications of the ACM, 60(6): 84–90. https://doi.org/10.1145/3065386

Kumar A (2018). Toward more accurate matching of contactless palmprint images under less constrained environments? IEEE Transactions on Information Forensics and Security, 14(1): 34-47. https://doi.org/10.1109/TIFS.2018.2837669

Kumar VN and Srinivasan B (2012). Ear biometrics in human identification system. International Journal of Information Technology and Computer Science, 2: 41-47. https://doi.org/10.5815/ijitcs.2012.02.06

Liu N, Liu J, Sun Z, and Tan T (2017). A code-level approach to heterogeneous iris recognition. IEEE Transactions on

Information Forensics and Security, 12(10): 2373-2386. https://doi.org/10.1109/TIFS.2017.2686013

Melekhov I, Kannala J, and Rahtu E (2016). Siamese network features for image matching. In the 23rd International Conference on Pattern Recognition, IEEE, Cancun, Mexico: 378-383. https://doi.org/10.1109/ICPR.2016.7899663

Meraoumia A, Kadri F, Bendjenna H, Chitroub S, and Bouridane A (2017). Improving biometric identification performance using PCANet deep learning and multispectral palmprint. In: Jiang R, Al-maadeed S, Bouridane A, Crookes P, and Beghdadi A (Eds.), Biometric security and privacy: 51-69. Springer, Cham, Switzerland. https://doi.org/10.1007/978-3-319-47301-7_3

Moridani MK, Moridani AK, and Gholipour M (2020). Powerful processing to three-dimensional facial recognition using triple information. International Journal of Advances in Applied Sciences, 9(4): 326–332. https://doi.org/10.11591/ijaas.v9.i4.pp326-332

Ramachandra R, Raja KB, Venkatesh S, Hegde S, Dandappanavar SD, and Busch C (2018). Verifying the newborns without infection risks using contactless palm prints. In the International Conference on Biometrics, IEEE, Gold Coast, Australia: 209-216. https://doi.org/10.1109/ICB2018.2018.00040

Ramachandran P, Zoph B, and Le QV (2017). Searching for activation functions. Available online at: https://arxiv.org/abs/1710.05941v2

Rezende E, Ruppert G, Carvalho T, Theophilo A, Ramos F, and de Geus P (2018). Malicious software classification using VGG16 deep neural network's bottleneck features. In: Latifi S (Ed.), Information technology-new generations: 51-59. Springer, Cham, Switzerland. https://doi.org/10.1007/978-3-319-77028-4_9

Rivaldería N, Gutiérrez-Redomero E, Alonso-Rodríguez C, Dipierri JE, and Martín LM (2017). Study of fingerprints in Argentina population for application in personal identification. Science and Justice, 57(3): 199-208. https://doi.org/10.1016/j.scijus.2017.02.004 **PMid:28454629**

Saied M, Elshenawy A, and Ezz MM (2020). A novel approach for improving dynamic biometric authentication and verification of human using eye blinking movement. Wireless Personal Communications, 115(1): 859-876. https://doi.org/10.1007/s11277-020-07601-x

Saqib S and Kazmi SAR (2018). Recognition of static gestures using correlation and cross-correlation. International Journal of Advances in Applied Sciences, 5(6): 11-18. https://doi.org/10.21833/ijaas.2018.06.002

Shao H, Zhong D, and Du X (2019). Efficient deep palmprint recognition via distilled hashing coding. In the IEEE/CVF Conference on Computer Vision and Pattern Recognition Workshops, Long Beach, USA. https://doi.org/10.1109/CVPRW.2019.00098

Simonyan K and Zisserman A (2015). Very deep convolutional networks for large-scale image recognition. In the 3rd International Conference on Learning Representations, San Diego, USA: 1-14. Available online at: https://arxiv.org/abs/1409.1556v6

Sun Z, Tan T, Wang Y, and Li SZ (2005). Ordinal palmprint representation for personal identification [representation read representation]. In the IEEE Computer Society Conference on Computer Vision and Pattern Recognition (CVPR'05), IEEE, San Diego, USA: 279-284. https://doi.org/10.1109/CVPR.2005.267

Tarawneh AS, Chetverikov D, and Hassanat AB (2018). Pilot comparative study of different deep features for palmprint identification in low-quality images. In the 9th Hungarian Conference on Computer Graphics and Geometry, Budapest, Hungary: 1-6. Available online at: https://arxiv.org/abs/1804.04602v1

Wang L and Geng X (2009). Behavioral biometrics for human identification: Intelligent applications. IGI Global, Pennsylvania, USA. https://doi.org/10.4018/978-1-60566-725-6

Zhang D, Guo Z, Lu G, Zhang L, and Zuo W (2009). An online system of multispectral palmprint verification. IEEE Transactions on Instrumentation and Measurement, 59(2): 480-490. https://doi.org/10.1109/TIM.2009.2028772

Zhang D, Zuo W, and Yue F (2012). A comparative study of palmprint recognition algorithms. ACM Computing Surveys (CSUR), 44(1): 1-37. https://doi.org/10.1145/2071389.2071391

Zhang L, Li L, Yang A, Shen Y, and Yang M (2017). Towards contactless palmprint recognition: A novel device, a new benchmark, and a collaborative representation based identification approach. Pattern Recognition, 69: 199-212. https://doi.org/10.1016/j.patcog.2017.04.016

Zhang Y, Zhang L, Liu X, Zhao S, Shen Y, and Yang Y (2019). Pay by showing your palm: A study of palmprint verification on mobile platforms. In the IEEE International Conference on Multimedia and Expo (ICME), IEEE, Shanghai, China: 862-867. https://doi.org/10.1109/ICME.2019.00153

Zhong D, Yang Y, and Du X (2018). Palmprint recognition using siamese network. In the Chinese Conference on Biometric Recognition, Urumchi, China: 48-55. https://doi.org/10.1007/978-3-319-97909-0_6